The inertial effect on the natural convection flow within a fluid-saturated porous medium

D. M. Manole and J. L. Lage
Mechanical Engineering Department, Southern Methodist University, Dallas, TX, USA

The general momentum equation for fluid flow within a porous medium is supposedly valid for any fluid–porous medium configuration. One of the main concerns of using the general equations refers to the inclusion of both inertia terms, namely, the convective inertia term and the Forchheimer term. In this study, we go beyond the important discussion about the correctness of including both terms in the general momentum equations by focusing upon the effect of the convective inertia term on the heat transfer results. The fluid–porous medium system considered here is a cavity bounded by solid surfaces with vertical walls maintained at constant but different temperatures. The natural convection problem is solved numerically, and the results are compared with a general theory developed by using the method of scale analysis. It is demonstrated that the convective inertia term effect upon the heat transfer results is minor for $0.01 \leq Pr \leq 1$, $10 \leq Ra_D \leq 10^4$, $10^{-8} \leq Da < 10^{-2}$, and porosities 0.4 and 0.8. It is also shown that, contrary to the general belief, the convective inertial effect upon the heat transfer within the cavity is minimized when the Prandtl number is reduced.

Keywords: porous medium; inertial effect; natural convection

Introduction

Five major steps can be recognized from an overview of the chronological evolution of fluid flow within a saturated porous medium theory.

The first and most basic step is the empirical model introduced by Darcy (1856). His model, known as Darcy's law, consists of a linear relationship between the unidirectional fluid velocity and the pressure gradient in the direction of the flow. It has been verified that Darcy's law is valid only when the Reynolds number based upon the volume-averaged velocity and the pore diameter is O(1) or smaller.

The range of applicability of Darcy's law was extended in a second major step by Dupuit (1863), although in the archival literature this extension is usually associated with the work by Forchheimer (1901). The nonlinear relationship between fluid velocity and pressure gradient verified experimentally for large Reynolds numbers was modeled by adding higher-order velocity terms to the Darcy equation.

Next, the friction effect of the interaction fluid–solid was investigated by Brinkman (1947). The procedure followed by Brinkman consists of using the expression for the drag force on a single sphere immersed within a flow of fluid. With this expression, the total force acting on a packed bed of spheres is then matched with the Darcy bulk frictional drag. The analysis results in the inclusion of a friction term proportional to the Laplacian of the fluid velocity in the Darcy equation.

The first three steps are brought together in a single momentum equation referred to in the literature as the Brinkman–Forchheimer–extended Darcy model for fluid flow through a porous medium.

A fourth step can be identified by the model presented by Wooding (1957), where the convective inertia term in the divergence form is added to the Darcy equation. The inconsistency of using the convective inertia term with the available number of boundary conditions from the basic Darcy equation was noted by Beck (1972). In modeling the inertial effect, Beck (1972) recommended the use of a quadratic velocity term only, in line with what was proposed by Forchheimer (1901).

The last step was the introduction of a general momentum equation for fluid flow through a porous medium. Vafai and Tien (1981) introduced the general equation for forced-convection heat transfer within a bounded porous medium. The general momentum equation include the convective inertia term, the pressure gradient term, the Brinkman and Forchheimer terms, and the Darcy term. However, in the analysis of Vafai and Tien, the convective inertia term was later neglected by using scale analysis arguments.

Recently, the complete general equation was formally derived by Hsu and Cheng (1990) for studying thermal dispersion in porous media. The applicability of this equation is supposed to range from a low-permeability porous medium configuration to a clear fluid configuration (in the present context, *clear* refers to a configuration with no porous matrix).

It is noteworthy that by including the Brinkman term, the general equation accommodates the convective inertia term as proposed by Wooding (1957). The nonslip boundary condition that comes together with the Brinkman term fulfills the requirement pointed out by Beck (1972). In conclusion, the general equation incorporates the previous three major steps, namely, the Forchheimer, Brinkman, and Wooding models, into the basic Darcy equation.

Address reprint requests to Professor Lage at the Mechanical Engineering Department, Southern Methodist University, Dallas, TX 75275-0335, USA.

Received 10 August 1992; accepted 8 April 1993

Although it seemed to be a settled issue, the application of the general momentum equation for modeling fluid flow through a porous medium is still a topic of controversy. For instance, the inclusion of the convective inertia term in the general equation was considered inappropriate by Joseph et al. (1982). They reasoned that the inertial effect is already accounted for by the Forchheimer term. However, within the past ten years, a large number of studies have been performed by using the general equation (with both inertia terms!) to model convective heat transfer within fluid-saturated porous media. For an up-to-date review of this subject, see Nield and Bejan (1991).

The indiscriminate use of the general equation for numerical modeling also has to be questioned regarding the computational costs associated with it. For instance, Lage (1992) showed for the case of Bénard convection that the inclusion of the convective inertia term has no effect upon the heat transfer results for a wide range of parameters. Considering that the convective inertia term is highly nonlinear, its inclusion becomes a costly overpowering of the mathematical model.

The tendency for universal use of the general momentum equation can be partially explained by the lack of experimental evidence to strengthen or to rebut this model. Furthermore, the similarity between the general equation for flow through a porous medium and the equation of motion in a clear fluid medium is very convenient from a numerical point of view. For instance, it makes it easier for the numerical analyst to solve problems where both media are present in the same control volume.

The almost nonexistent emphasis in the heat transfer literature about the limitations of the general momentum equation was recently pointed out by Nield (1991). These limitations are related to the local time-derivative inertia term, the viscous Brinkman term, and the convective inertia term. The first of these is important only when imposed transients (e.g., oscillatory pressure gradient) are of interest. The last two are somewhat related: the extra boundary condition needed for the inclusion of the convective inertia term comes *with* the Brinkman term. So, from a mathematical point of view, there is no sense in arguing about the inclusion of the convective inertia term unless the Brinkman term is also included. The opposite, however, is not necessarily the case, since the Brinkman term can be included in the equation of motion regardless of the inclusion of the convective inertia term.

The limitations on Brinkman's procedure, according to Nield (1991), are mainly two: the necessity for including Brinkman term is inconsistent for porosities smaller than about 0.6; and the viscous effect (justification used for including the Brinkman term) is restricted to within a small distance from the solid boundaries, so its effect might be neglected.

The first argument can be easily accepted, although, as also pointed out by Nield (1991), practical situations of interest where high-porosity media are present do exist and have attracted increased interest (Bejan and Lage, 1991; Lee and Howell, 1991; Lage and Bejan, 1991).

The second argument, although correct, is not general. For instance, in natural convection flow within a porous medium cavity heated or cooled from the sides, the region closest to the solid boundaries is the one that dictates the heat transfer mechanism within the cavity (Bejan and Poulikakos, 1984; Poulikakos, 1985). For this fundamental problem, it becomes difficult to justify the neglect of the Brinkman term. Interestingly, the same argument was used by Vafai and Tien (1981) to justify the inclusion of the Brinkman term in the Forchheimer-extended Darcy equation for forced-convection heat transfer.

A very stimulating study by Ettefagh et al. (1991) established, for the first time, the individual effects of several flow models—namely, Darcy, Forchheimer-extended Darcy, Brinkman-extended Darcy, and generalized—on the natural convection flow within open-ended cavities. It was shown that, for the specific configuration studied, the Brinkman term can have a definite influence on the flow for Darcy numbers as low as 10^{-4}. The importance of including the convective inertia term for low Prandtl number media was also pointed out.

The answer to the question of when the convective inertia term should be included for modeling natural convection flow is still not clear. In the present work we do not attempt to answer this fundamental question in its entirety. We do, however, establish a range within which the use of the

Notation

Da	Darcy number, Equation 5
F	Nondimensional inertia coefficient, Equation 5
g	Gravity acceleration, m/s^2
H	Height of the porous cavity, m
k	Thermal conductivity, W/m K
K	Permeability, m^2
Nu	Nusselt number
p	Pressure, Pa
P	Nondimensional pressure, Equation 5
Pr	Prandtl number, Equation 5
q''	Heat flux, W/m^2
Ra	Rayleigh number, Equation 5
T	Temperature, K
u, v	Horizontal and vertical velocity components, m/s
x, y	Horizontal and vertical coordinates, m
U, V	Nondimensional velocity components, Equation 5
X, Y	Nondimensional coordinates, Equation 5

Greek symbols

α	Thermal diffusivity, m^2/s
α	Rate of grid stretching, Equation 8
β	Isobaric coefficient of thermal expansion, K^{-1}
δ	Length scale
Δ	Grid base, Equation 8
θ	Nondimensional temperature, Equation 5
ν	Kinematic viscosity, m^2/s
ρ	Density, kg/m^3
ϕ	Porosity

Subscripts

avg	Wall averaged, Equation 9
c	Cold, Equation 5
D	Darcy-modified, Equation 10
f	Fluid, Equation 5
h	Hot, Equation 5
m	Porous medium (fluid and solid matrix), Equation 5
s	Stretching, Equation 8
θ	Related to temperature, Equation 5

convective inertia term becomes irrelevant for modeling natural convection within a porous medium heated from the sides. In such a range, the choice of including or not including the convective inertia term is a trade-off between the convenience of programming and the computer cost associated with solving the more complicated model.

Equations of motion

The basic configuration shown in Figure 1 is a cross section of a fluid-saturated porous medium cavity with top and bottom adiabatic walls. The porous medium is assumed to have constant porosity, so the possibility of porosity variation near the walls (channeling) is neglected. The walls of the cavity are assumed to be impermeable, with the vertical walls being isothermal.

To verify the influence of the convective inertia term, the Brinkman term has to be included in the momentum equation. For simplicity, the effective viscosity is assumed to be equal to the fluid viscosity divided by the solid matrix porosity.

The general nondimensional set of equations (Vafai and Tien 1981) that governs the steady-state fluid motion within the cavity is

$$\frac{\partial U}{\partial X}+\frac{\partial V}{\partial Y}=0 \tag{1}$$

$$\tilde{V}\cdot\nabla U=-\frac{\partial P}{\partial X}+\phi\mathrm{Pr}\,\nabla^2 U-\frac{\phi^2 F}{\mathrm{Da}}|\tilde{V}|U-\frac{\phi^2\mathrm{Pr}}{\mathrm{Da}}U \tag{2}$$

$$\tilde{V}\cdot\nabla V=-\frac{\partial P}{\partial Y}+\phi\mathrm{Pr}\,\nabla^2 V-\frac{\phi^2 F}{\mathrm{Da}}|\tilde{V}|V-\frac{\phi^2\mathrm{Pr}}{\mathrm{Da}}V+\phi^2\mathrm{Ra}\mathrm{Pr}\,\theta \tag{3}$$

$$\tilde{V}\cdot\nabla\theta=\nabla^2\theta \tag{4}$$

where $\tilde{V}$ is the vector velocity with horizontal, U, and vertical, V, components, and absolute value, $|\tilde{V}|$, equal to $\sqrt{U^2+V^2}$. The gradient and the Laplacian operators, in Cartesian coordinates, are $\nabla=\partial/\partial X\tilde{i}+\partial/\partial Y\tilde{j}$ and $\nabla^2=\partial^2/\partial X^2+\partial^2/\partial Y^2$.

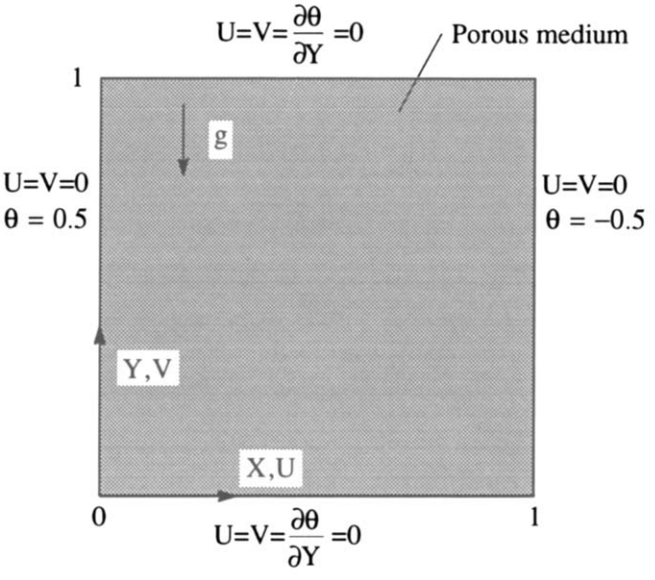

Figure 1 Two-dimensional fluid-saturated porous medium cavity with velocity and temperature boundary conditions

The boundary conditions required to solve Equations 1 to 4 are also depicted in Figure 1.

From left to right, the momentum equation (3) represents the balance among the following terms: convective inertia, pressure, Brinkman, Forchheimer, Darcy, and buoyancy.

The present mathematical model assumes constant thermophysical properties, with the saturating fluid being of the Boussinesq–Oberbeck type. Also, the fluid and the porous matrix are assumed to be in local thermodynamic equilibrium.

The dimensional variables and properties (listed in the nomenclature) are related to the nondimensional variables through the following relations:

$$(X,Y)=\frac{(x,y)}{H},\qquad (U,V)=\frac{(u,v)}{(\alpha_m/H)},$$

$$\theta=\frac{T-(T_h+T_c)/2}{T_h-T_c},\qquad P=\frac{\phi^2H^2(p+\rho_f gy)}{\rho_f\alpha_m^2},$$

$$F=1.75\left(\frac{\mathrm{Da}}{150\phi^3}\right)^{1/2},$$

$$\mathrm{Da}=\frac{K}{H^2},\qquad \mathrm{Pr}=\frac{\nu}{\alpha_m},\qquad \mathrm{Ra}=\frac{g\beta H^3(T_h-T_c)}{\nu\alpha_m}. \tag{5}$$

The Ergun (1952) model is already implemented when defining the nondimensional inertia coefficient, F, as shown in Equation 5. The independent nondimensional parameters that govern the heat transfer process within the cavity are the modified Prandtl number, Pr, the Rayleigh number, Ra, the Darcy number, Da, and the porosity of the solid matrix, ϕ.

The effects of the convective inertia term are obtained by comparing the results obtained by using the set of general equations with the results obtained by neglecting the convective inertia term from Equations 2 and 3.

Numerical method

The numerical method chosen for this investigation is the finite-volume method (Patankar, 1980). Discretized (algebraic) equations are obtained by integrating the governing equations 1–4 over small control volumes. A power-law scheme, based on the local Péclet number, is used to complete the discretization. The resulting set of algebraic equations with proper boundary conditions is solved by the Tri-Diagonal-Matrix-Algorithm in a line-by-line fashion.

The convergence of the numerical solution is monitored locally by the maximum absolute temperature change and by the maximum relative velocity change between two consecutive iterations, i and $i+1$, respectively:

$$\mathrm{MAX}|(\theta)^{i+1}-(\theta)^i|<10^{-5} \tag{6}$$

$$\mathrm{MAX}\left|\frac{(U,V)^{i+1}-(U,V)^i}{(U,V)^i}\right|<10^{-6} \tag{7}$$

The absolute error used for the temperature convergence criterion as shown by Equation 6, although not common, is found to be much more precise for the present case. The relative error expression of Equation 7 cannot be used when the local value of the variable at iteration i is zero. However, the temperature inside the enclosure is bounded by the limits 0.5 and −0.5 at the vertical boundaries, so Equation 6 guarantees that the temperature values are converged to within at least 6 significant digits.

The numerical grid is nonuniform and symmetric in both directions. The grid lines are distributed starting from the

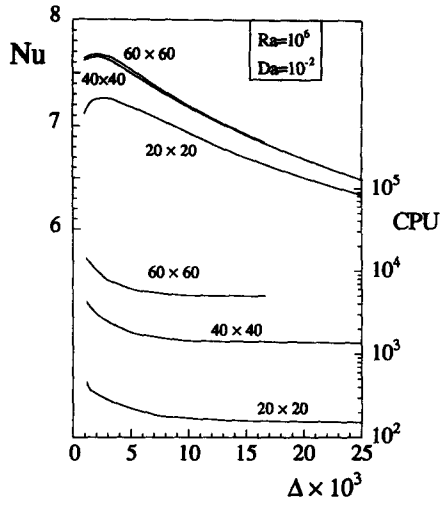

Figure 2 Grid accuracy test with corresponding total computer time

boundaries up to the center of the domain, following the power rule

$$s_{j+1} = s_j + \alpha_s^j \Delta \tag{8}$$

where s_j is the spatial location of the j^{th} grid line (s_j is measured away from the boundary), and α_s and Δ are, respectively, the rate of grid stretching and the spacing between the first grid line and the boundary (base).

Grid accuracy tests are based upon the Nusselt number defined as the nondimensional wall-averaged heat flux,

$$\mathrm{Nu} = \frac{q''_{avg} H}{k_m (T_h - T_c)} = -\int_0^1 \left(\frac{\partial \theta}{\partial X}\right)_{X=0 \text{ or } 1} dY \tag{9}$$

Tests are performed following the guidelines presented by Manole and Lage (1993). For instance, we present in Figure 2 the results of the accuracy tests for the case $\mathrm{Ra} = 10^6$, $\mathrm{Pr} = 1$, $\mathrm{Da} = 10^{-2}$, and porosity equal to 0.4. The three curves in the top half of the graph present the Nusselt number variation with the grid base, Δ, for 20 x 20, 40 x 40, and 60 x 60 grid lines. The corresponding computer time, in CPU seconds of a DEC 5000-240 workstation, is shown by the three curves in the lower half of the figure. For the present case, a 60 x 60 grid is chosen with the grid base value, Δ, equal to 2.5×10^{-3}.

The present computer program is also validated against the results reported by Ettefagh et al. (1991) for several different cases using the Forchheimer-extended and the Brinkman-extended Darcy models. The Nusselt numbers differ by less than 4 percent. For the Darcy model, a comparison with the available results from the literature was reported by Manole and Lage (1993).

Numerical results

In the present study, the following ranges are investigated: $10^{-8} \leq \mathrm{Da} \leq 10^{-2}$, $0.01 \leq \mathrm{Pr} \leq 1$, and $10 \leq \mathrm{Ra_D} \leq 10^4$.

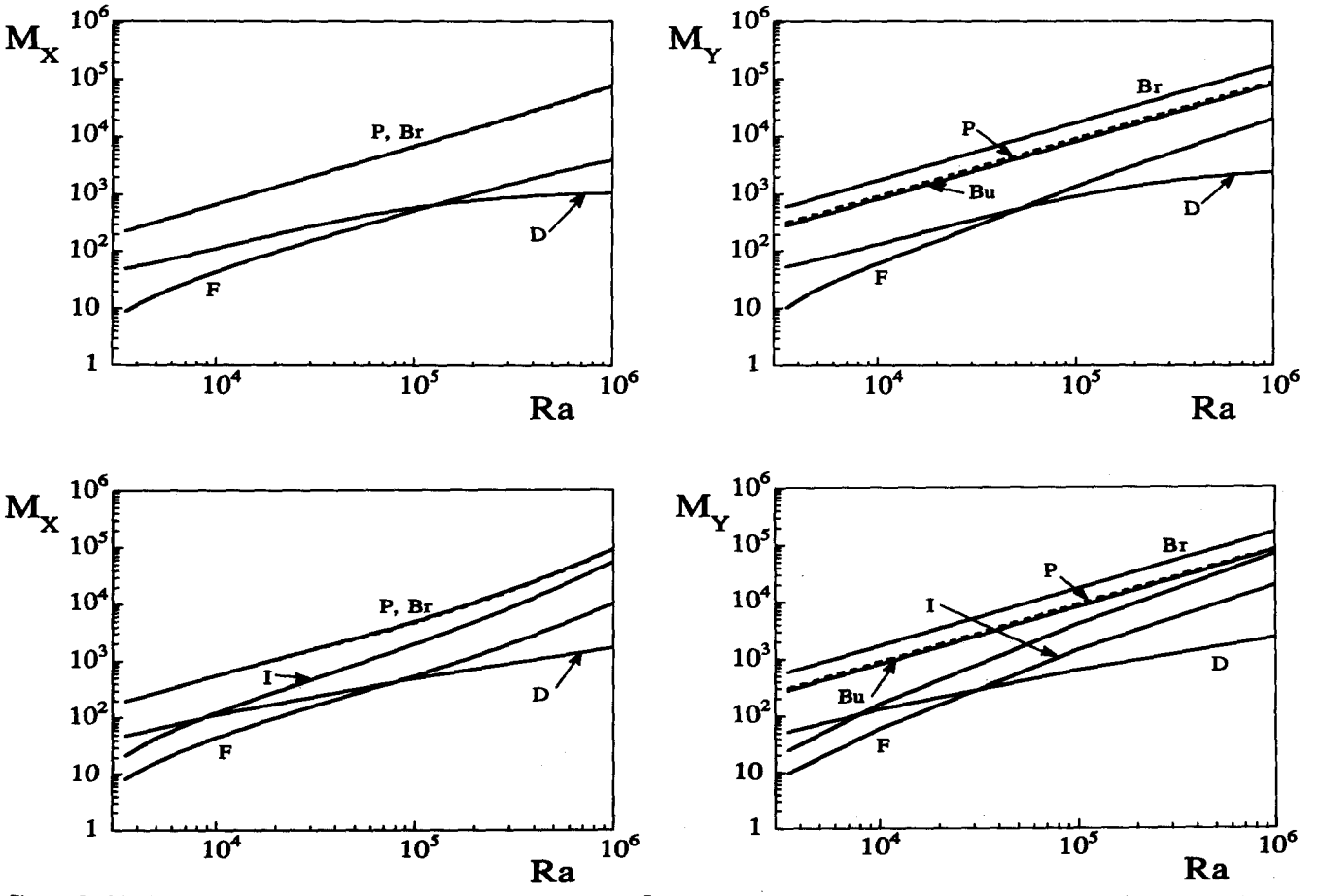

Figure 3 Maxima of momentum terms: *P*—pressure, Br—Brinkman, Bu—buoyancy, D—Darcy, F—Forchheimer, I—convective inertia. $\phi = 0.4$, $\mathrm{Pr} = 1$, $\mathrm{Da} = 10^{-2}$. The top graphs neglect the convective inertia term; the bottom graphs include the convective inertia term

The Darcy-modified Rayleigh number, Ra_D,

$$Ra_D = RaDa \tag{10}$$

is a new parameter that becomes increasingly important as the Darcy number is reduced. In fact, when $Da \rightarrow 0$, Ra_D becomes the only parameter to influence the solution of Equations 1–4.

The representative porosity values of 0.4 and 0.8 are used to investigate how the porosity affects the convective inertial heat transfer effects.

The strategy used by Lage (1992) is followed here to check the effect of the convective inertia term. After obtaining the numerical results for a specific case, the maximum values for each of the terms of the momentum equations 2 and 3 are found within the numerical domain. The procedure is then repeated for the same case neglecting the convective inertia term from Equations 2 and 3.

For Darcy number equal to 10^{-2}, Prandtl number equal to 1, and porosity equal to 0.4, Figure 3 compares each term of the horizontal momentum equation, M_X, and of the vertical momentum equation, M_Y. The top graphs are obtained by neglecting the convective inertia term from the momentum equations, while the bottom graphs are obtained by including it. The results for the smaller Darcy number investigated here, $Da = 10^{-8}$, are presented in Figure 4.

It can be observed in Figure 3 that the Darcy, D, and the Forchheimer, F, terms are consistently smaller than the pressure term. As expected, the convective inertia term, I, increases in importance as the Rayleigh number is increased. Although the same observation can be extended for the Darcy and the Forchheimer terms, their rates of increase are smaller.

The graphs on the right side of Figure 3 show the crossing between the maxima of the Forchheimer term and the maxima of the Darcy term. For Rayleigh number greater than approximately 3×10^4, the Darcy term becomes progressively smaller than the Forchheimer term. This could indicate the flow switching from the Darcy regime to the Forchheimer regime. Note, however, that the maxima of both terms are at least one order of magnitude smaller than the maxima of the pressure term, P, for the whole Rayleigh range.

The convective inertia term effect upon the other momentum terms seems to be minor when the top and bottom graphs of Figure 3 are compared.

The effect of the convective inertia term upon the other terms is even smaller, if not negligible, when the Darcy number is reduced (Figure 4), being noticed only upon the horizontal Brinkman momentum term, Br. For this case the maxima of the Forchheimer term no longer crosses the maxima of the Darcy term, with the Forchheimer term being consistently smaller.

One important aspect to note from both Figures 3 and 4 for the vertical momentum terms, M_Y, is the almost perfect matching between the maxima of the pressure gradient term, P, and the maxima of the buoyancy term, Bu. This important

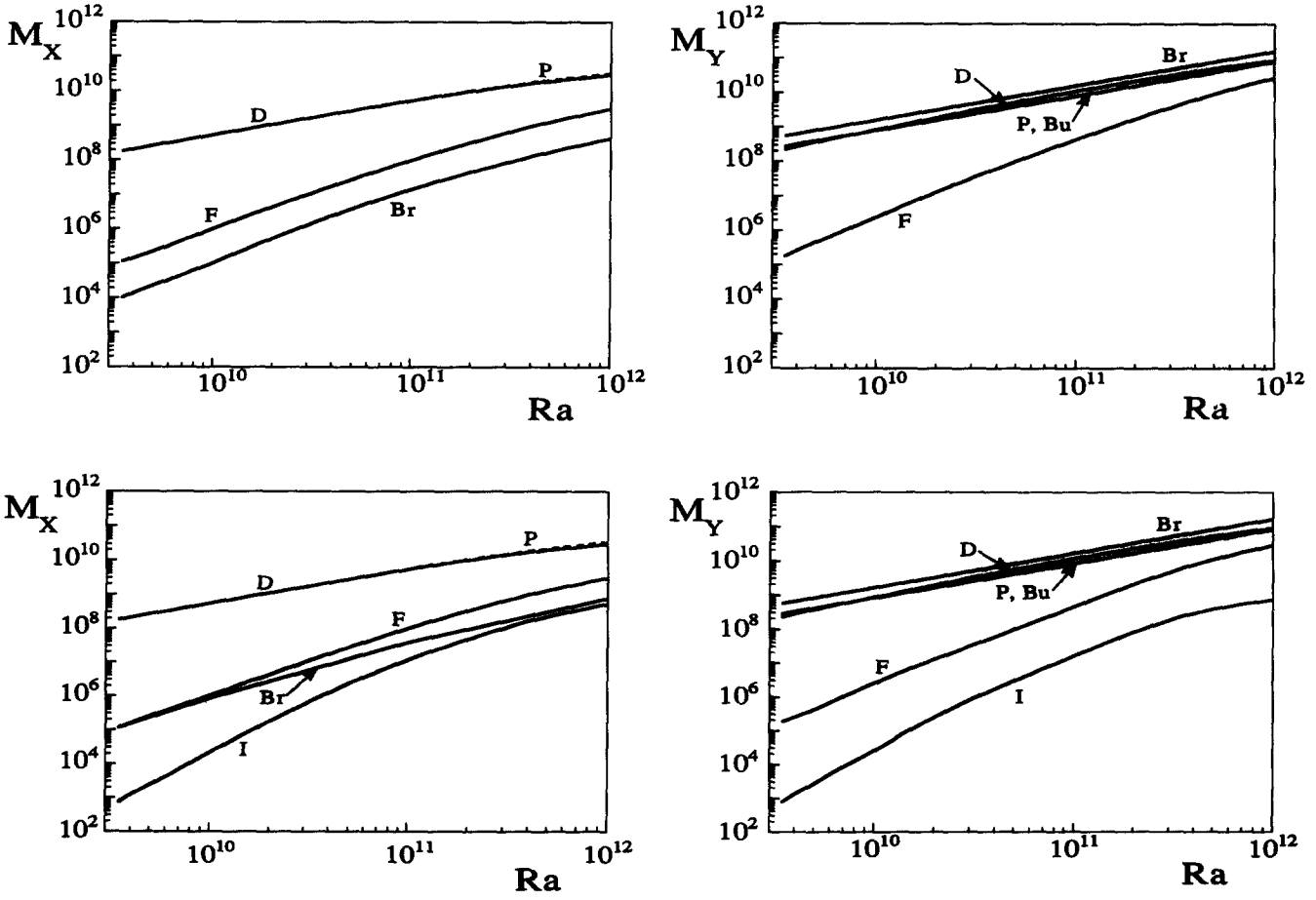

Figure 4 Maxima of momentum terms: P—pressure, Br—Brinkman, Bu—buoyancy, D—Darcy, F—Forchheimer, I—convective inertia. $\phi = 0.4$, $Pr = 1$, $Da = 10^{-8}$. The top graphs neglect the convective inertia term; the bottom graphs include the convective inertia term

observation, obtained numerically, is used to simplify the theoretical considerations presented in the next section.

The different magnitudes of the convective inertia term are compared in Figure 5. The Darcy-modified inertia term, I_D, defined as the maximum inertia term value multiplied by the corresponding Darcy number, is plotted against the Darcy-modified Rayleigh number, Ra_D. It can be seen that the value of the convective inertia term, in both directions, increases by a factor of 10 when the Darcy number is increased from 10^{-6} to 10^{-2}. Not plotted in Figure 5 are the results for the case $Da = 10^{-8}$ when the value of the convective inertia term is negligible.

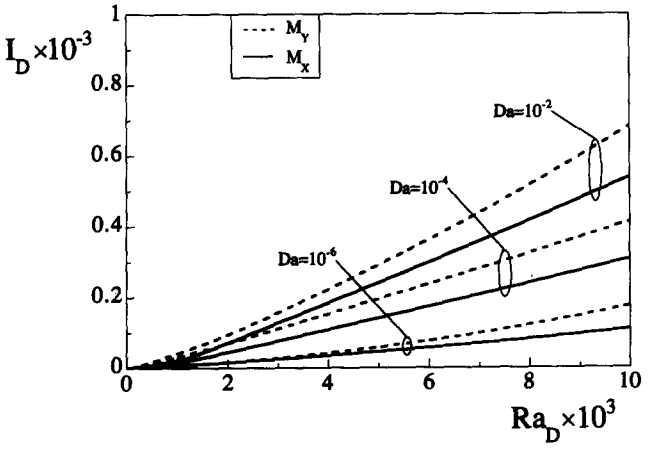

Figure 5 Maximum values for the horizontal, M_X, and vertical, M_Y, momentum equation convective inertia terms. Pr = 1 and $\phi = 0.4$

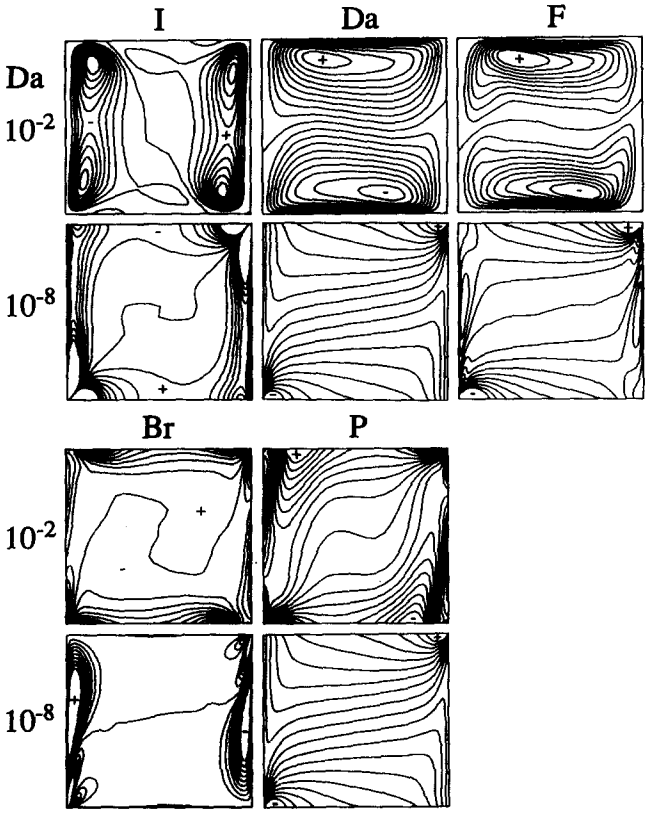

Figure 6 Isolines of the horizontal direction momentum equation terms. $\phi = 0.4$, Pr = 1, $Ra_D = 10^4$

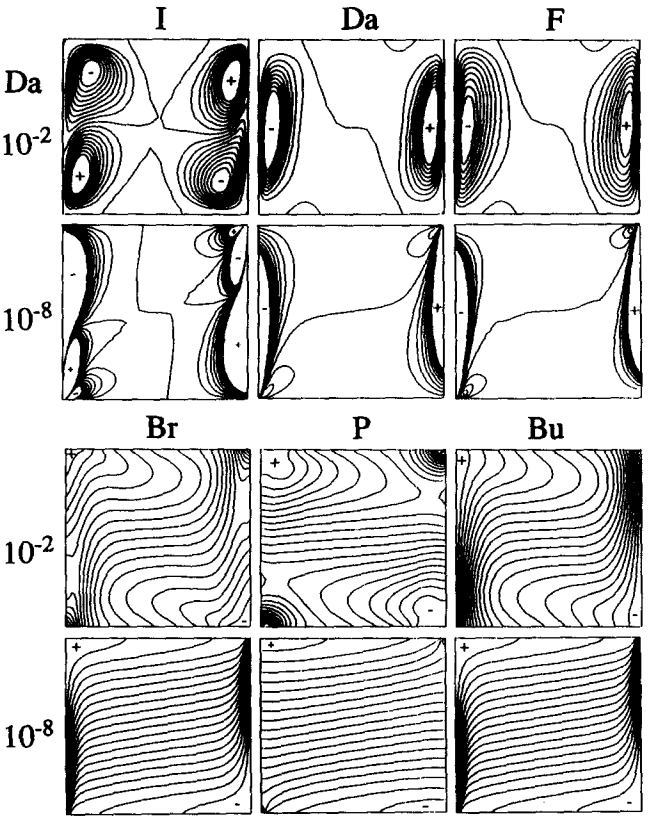

Figure 7 Isolines of the vertical direction momentum equation terms. $\phi = 0.4$, Pr = 1, $Ra_D = 10^4$

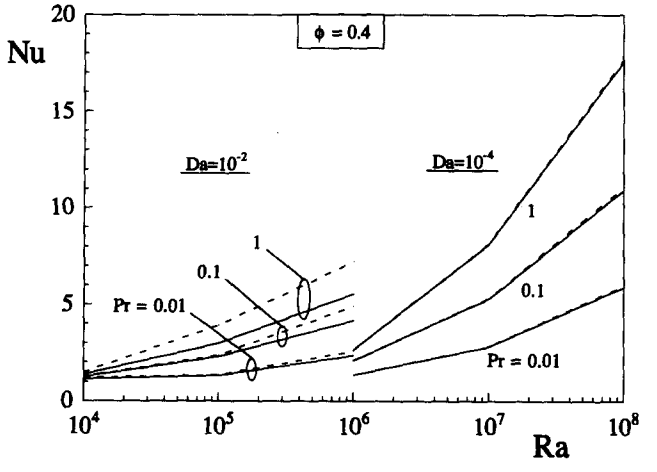

Figure 8 Porosity effect on the numerical Nusselt number obtained by including convective inertia term (dashed line) and by neglecting the convective inertia term (continuous line)

Figures 6 and 7 present the isolines for all the terms of the momentum equations for $Ra_D = 10^3$, and $Da = 10^{-2}$ and $Da = 10^{-8}$, respectively. As noted before in the analysis of Figures 3 and 4 for the vertical momentum terms, there is a strong similarity between the isolines of the buoyancy term and the isolines of the pressure term.

The isolines of the convective inertia term show the locations of the acceleration and deceleration of the flow. For instance, in the Y-direction (Figure 7) for $Da = 10^{-2}$, starting from the

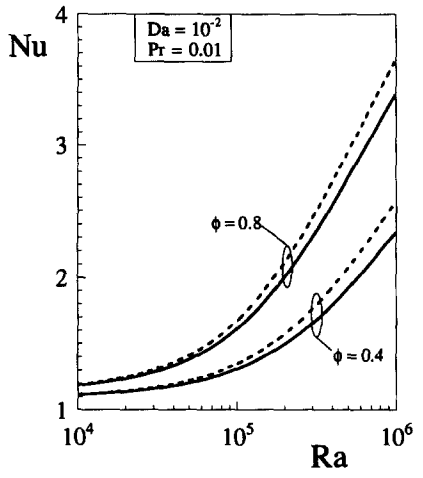

Figure 9 Darcy and Prandtl numbers effect on the numerical Nusselt number obtained by including convective inertia term (dashed line) and by neglecting the convective inertia term (continuous line)

lower left corner, the fluid accelerates upwards, moving close by the hot vertical wall. Near the mid-height of the wall, the flow starts to decelerate towards the upper left corner. The process is reversed in the cold vertical wall.

Figure 8 shows the direct effect of the convective inertia term upon the Nusselt number. The dashed lines are obtained by neglecting the convective inertia term from Equations 2 and 3. The inertial effect increases with Darcy, being noticeable for $Da = 10^{-2}$ or larger. A somewhat unexpected result is the Prandtl number effect: the convective inertial effect is reduced with the decrease of the Prandtl number. To investigate if this is the case also for a high- porosity medium, results for $\phi = 0.8$, $Pr = 0.01$, and $Da = 10^{-2}$ are obtained and presented in Figure 9. Indeed, the relative convective inertial effect is roughly the same for both porosities.

Theoretical analysis

The effective range of the convective inertia term can be predicted theoretically by first writing the momentum equation in the Y-direction, Equation 3, in a scaling form:

$$V^2 \sim -\Delta P,\ -\phi \mathrm{Pr}\,\frac{V}{\delta^2},\ -\frac{\phi^2 F}{\mathrm{Da}}V^2,\ -\frac{\phi^2 \mathrm{Pr}}{\mathrm{Da}}V,\ \phi^2 \mathrm{RaPr}\,\theta \quad (11)$$

For fluid-saturated porous media with Prandtl number greater than 1, Equation 4 gives the proper scale for δ as $V^{-1/2}$ (note in this case (Bejan 1984), that the thermal boundary-layer thickness, δ_θ, that appears in Equation 4 scales with the distance between wall and velocity peak, δ). Equation 11 can then be written, relative to the scale of the convective inertia term, as

$$1 \sim -\phi\,\mathrm{Pr},\ -\frac{0.143\phi^{1/2}}{\mathrm{Da}^{1/2}},\ -\frac{\mathrm{Pr}\,\phi^2}{V\,\mathrm{Da}},\ \frac{\phi^2}{2V^2}\,\mathrm{RaPr} \quad (12)$$

In line with the numerical results presented previously, the pressure gradient term, ΔP, of Equation 11 is assumed to have the same scale as the buoyancy term, $\phi^2 \mathrm{RaPr}\theta$, so it is neglected in Equation 12. This simplifies the analysis by avoiding the usual cross-differentiation of the momentum equations 2 and 3 to cancel the pressure gradient term. Also, the inertia coefficient, F, of Equation 11 is replaced by the relation shown in Equation 5, and the nondimensional temperature scale, θ, is replaced by 0.5.

Equation 12 reads, from left to right, a balance between the following terms: inertia, Brinkman, Forchheimer, Darcy, and buoyancy. The only term that cannot be neglected in any circumstances is the buoyancy term, the "motto" of the natural convection phenomenon.

An equivalent of Equation 12 for systems with porous Prandtl number O(1) or smaller (in this case (Bejan 1984), the thermal boundary-layer thickness in Equation 4 scales with $\delta/\mathrm{Pr}^{1/2}$), can be obtained by simply substituting the scale of δ in Equation 11 by

$$\delta \sim \left(\frac{\mathrm{Pr}}{V}\right)^{1/2} \quad (13)$$

Equation 12 can be used to find a general expression for the velocity scale. Solving the quadratic equation in V and discarding the negative root (remember that by using $\theta \sim 0.5$ it is implicit that the scale analysis is being peformed within a region close to the hot wall where $V > 0$), the velocity scale is obtained as

$$V \sim \frac{-\dfrac{\mathrm{Pr}\,\phi^2}{\mathrm{Da}} + \left[\dfrac{\mathrm{Pr}^2\phi^4}{\mathrm{Da}^2} + 2\phi^2\,\mathrm{RaPr}\left(1 + \phi A(\mathrm{Pr})\mathrm{Pr} + \dfrac{0.143\phi^{1/2}}{\mathrm{Da}^{1/2}}\right)\right]^{1/2}}{2\left(1 + \phi A(\mathrm{Pr})\mathrm{Pr} + \dfrac{0.143\phi^{1/2}}{\mathrm{Da}^{1/2}}\right)} \quad (14)$$

The different scales for δ are accounted for in Equation 14 by the new function $A(\mathrm{Pr})$. For $\mathrm{Pr} \geq 1$, $A(\mathrm{Pr})$ is set equal to 1, and for $\mathrm{Pr} < 1$, $A(\mathrm{Pr})$ becomes equal to Pr^{-1}.

Equation 9 provides the Nusselt number scale

$$\mathrm{Nu} \sim \frac{1}{2\delta_\theta} \quad (15)$$

where, from scaling equation 4, $\delta_\theta \sim V^{-1/2}$, and therefore

$$\mathrm{Nu} \sim \frac{V^{1/2}}{2} \quad (16)$$

Combining Equations 14 and 16, a general correlation for the Nusselt number is found as

$$Nu \sim \frac{1}{2}\left\{\frac{-\dfrac{\mathrm{Pr}\,\phi^2}{\mathrm{Da}} + \left[\dfrac{\mathrm{Pr}^2\phi^4}{\mathrm{Da}^2} + 2\phi^2\,\mathrm{RaPr}\left(1 + \phi A(\mathrm{Pr})\mathrm{Pr} + \dfrac{0.143\phi^{1/2}}{\mathrm{Da}^{1/2}}\right)\right]^{1/2}}{2\left(1 + \phi A(\mathrm{Pr})\mathrm{Pr} + \dfrac{0.143\phi^{1/2}}{\mathrm{Da}^{1/2}}\right)}\right\}^{1/2} \quad (17)$$

Each group on the right side of Equation 17 refers to one term of the momentum equation 3. Within parentheses we have, from left to right, groups that refer to the convective inertia and the Brinkman and Forchheimer terms. In the numerator, multiplying the parentheses, we have the buoyancy group and the other two groups that refer to the Darcy term.

It is noteworthy that Equation 17 indeed reduces to the correct Nusselt number scale for the Forchheimer regime (Nield

and Bejan 1991) when the groups related to the Darcy, convective inertia, and Brinkman terms are set equal to zero:

$$\mathrm{Nu} \sim 0.684\phi^{3/8}\mathrm{Da}^{1/8}(\mathrm{RaPr})^{1/4} \tag{18}$$

The same is true for the clear fluid case when the groups relative to Darcy and Forchheimer terms are set equal to zero (Bejan 1984):

$$\mathrm{Nu} \sim 0.42\left(\frac{\mathrm{RaPr}}{1 + A(\mathrm{Pr})\mathrm{Pr}}\right)^{1/4} \tag{19}$$

The present theoretical analysis provides, for the first time, a general correlation for the Nusselt number that is valid for the entire range covered by the general equations 1–4.

Equation 17 can also be used to show when the convective inertia term of the momentum equations 2–3 affects the Nusselt number. This effect is shown in Figure 10, where the Nusselt number obtained by using Equation 17 is shown by continuous lines and the Nusselt number obtained after neglecting the convective inertia term in Equation 17 is plotted with dashed lines. The neglect of the convective inertia term is obtained by replacing the expressions within parentheses in Equation 17 by a different expression, as shown in Equation 20.

$$\left(1 + \phi A(\mathrm{Pr})\mathrm{Pr} + \frac{0.143\phi^{1/2}}{\mathrm{Da}^{1/2}}\right) \rightarrow \left(\phi A(\mathrm{Pr})\mathrm{Pr} + \frac{0.143\phi^{1/2}}{\mathrm{Da}^{1/2}}\right) \tag{20}$$

As can be observed from Figure 10, the important trends related to the convective inertia term obtained by the numerical calculations are indeed confirmed by the theoretical results. The agreement between the theoretical Nusselt numbers shown in Figure 10 and the numerical values presented in Figures 8 and 9 is notable.

For $\mathrm{Pr} < 1$, Equation 17 predicts a progressively smaller effect of the convective inertia term upon the Nusselt number when the Prandtl number is reduced. This tendency has also been highlighted during the analysis of the numerical results.

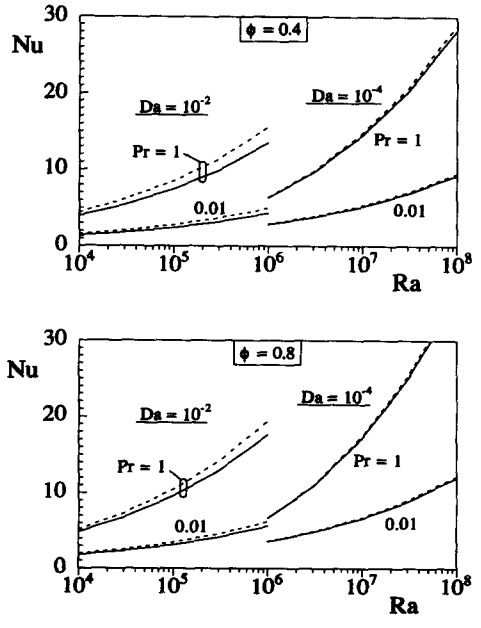

Figure 10 Theoretical results: porosity, Darcy, and Prandtl numbers' effect on the Nusselt number obtained by including the convective inertia term (dashed line) and by neglecting the convective inertia term (continuous line)

Final remarks

The numerical investigation reported here shows that the convective inertia term effect upon the heat transfer results is negligible for Darcy number smaller than 10^{-2}. Furthermore, by reducing the Prandtl number this effect is reduced even more.

The porosity of the medium has a minor influence on the inertial effect over the Nusselt number, the effect being slightly reduced when the porosity is increased.

From the numerical calculations, the largest discrepancy that is observed in the Nusselt number by not including the convective inertia term on the momentum equations is about 40 percent. This discrepancy is obtained for Prandtl number equal to 1 and Darcy number equal to 10^{-2}, with the Darcy-modified Rayleigh number being the largest investigated in here, equal to 10^4.

A theoretical study based on scale analysis strengthened the conclusions drawn from the numerical investigation. The qualitative agreement between theoretical results and numerical results is excellent.

The discussion about the correctness of including the convective inertia term in the momentum equation should be restricted to cases with large Darcy number, $\mathrm{Da} \geq 10^{-2}$, and large Prandtl numbers, $\mathrm{Pr} \geq 1$. However, at this high Darcy number, the medium might no longer be considered as porous, and the discussion becomes irrelevant.

Acknowledgments

The authors acknowledge with gratitude the support received from the School of Engineering and Applied Science of the Southern Methodist University. Constructive comments of one reviewer are also appreciated.

References

Beck, J. L. 1972. Convection in a box of porous material saturated with fluid. *Phys. Fluids*, **15**, 1377–1383

Bejan, A. 1984. *Convection Heat Transfer*. John Wiley & Sons, New York, ch. 4

Bejan, A. and Lage, J. L. 1991. Heat transfer from a surface covered with hair. In S. Kakaç, B. Kilkis, F. Arinç, and F. A. Kulacki (eds.), *NATO Advanced Study Institute: Convective Heat and Mass Transfer in Porous Media*. Kluwer, Dordrecht, The Netherlands

Bejan, A. and Poulikakos, D. 1984. The non-Darcy regime for vertical boundary layer convection in a porous medium. *Int. J. Heat Mass Transfer*, **27**, 717–722

Brinkman, H. C. 1947. A calculation of the viscous force exerted by a flowing fluid on a dense swarm of particles. *Appl. Sci. Res.*, **1**, 27–34

Darcy, H. 1856. *Les Fontaines Publiques de la Ville de Dijon*. Victor Dalmond, Paris

Dupuit, J. 1863. *Estudes Théoriques et Pratiques sur le Movement des Eaux*. Dunod, Paris

Ettefagh, J., Vafai, K., and Kim, S. J. 1991. Non-Darcian effects in open-ended cavities filled with a porous medium. *J. Heat Transfer*, **113**, 747–756

Ergun, S. 1952. Fluid flow through packed columns. *Chem. Eng. Prog.*, **48**, 89–94

Forchheimer, P. 1901. Wasserbewegung durch Boden. *Z. Ver. D. Ing.*, **45**, 1782–1788

Hsu, C. T. and Cheng, P. 1990. Thermal dispersion in a porous medium. *Int. J. Heat Mass Transfer*, **33**, 1587–1597

Joseph, D. D., Nield, D. A., and Papanicolaou, G. 1982. Nonlinear equation governing flow in a saturated porous medium. *Water Resources Res.*, **18**, 1049–1052

Lage, J. L. 1992. The effect of the convective inertial term on Benard convection in a porous medium. *Numer. Heat Transfer A*, **22**, 469–485

Lage, J. L. and Bejan, A. 1991. Natural convection from a vertical surface covered with hair. *Int. J. Heat Fluid Flow*, **12**, 46–53

Lee, K. and Howell, J. 1991. Theoretical and experimental heat and mass transfer in highly porous media. *Int. J. Heat Mass Transfer*, **34**, 2123–2132

Manole, D. M. and Lage, J. L. 1993. Nonuniform grid accuracy test applied to the natural convection flow within a porous medium cavity. *Numer. Heat Transfer B*, **23**, 351–368

Nield, D. A. and Bejan, A. 1991. *Convection in Porous Media*. Springer-Verlag, New York, ch. 7

Nield, D. A. 1991. The limitations of the Brinkman–Forchheimer equation in modeling flow in a saturated porous medium and at an interface. *Int. J. Heat Fluid Flow*, **12**, 269–272

Patankar, S. V. 1980. *Numerical Heat Transfer and Fluid Flow*. Hemisphere, Washington

Poulikakos, D. 1985. A departure from the Darcy model in boundary layer natural convection in a vertical porous layer with uniform heat flux from the side. *J. Heat Transfer*, **107**, 716–720

Vafai, K. and Tien, C. L. 1981. Boundary and inertia effects on flow and heat transfer in porous media. *Int. J. Heat Mass Transfer*, **24**, 195–203

Wooding, R. A. 1957. Steady state free thermal convection of liquid in a saturated permeable medium. *J. Fluid Mech.*, **2**, 273–285